



Case Study

Interpretation of geophysical and GIS-based remote sensing data for sustainable groundwater resource management in the basement of north-eastern Osun State, Nigeria

Dele Falebita¹  · Oluseyi Olajuyigbe¹ · S. Sunday Abeiya² · Oche Christopher³ · Ademola Aderoju¹

Received: 27 January 2020 / Accepted: 19 August 2020 / Published online: 31 August 2020
© Springer Nature Switzerland AG 2020

Abstract

This study describes the interpretation of integrated GIS-based remote sensing and electrical resistivity geophysical methods as part of the need to provide groundwater overview for sustainable management in the basement of north-eastern Osun State, Nigeria. Six groundwater conditioning factors are synthesized based on the analytical hierarchy process and multi-criteria decision analysis to produce groundwater potential index map constrained by existing borehole yields. The results indicate that the estimated groundwater potential index map can serve as a gross predictor of the groundwater distribution in the region. This study may influence town planning and land use decisions for sustainable management of groundwater resource in the area.

Keywords Sustainable groundwater management · Basement complex · GIS-based remote sensing · Surface geophysical · Nigeria

1 Introduction

The south-western Nigeria is underlain by widespread occurrence of about 80% impermeable crystalline rocks which makes groundwater exploitation challenging and limits groundwater availability [48]. However, studies have shown that storage and transmission of groundwater is greatly influenced by local and regional fractures [3, 59] which may be associated with zones of high permeability and concentrated groundwater flow [14, 18, 26]. So, the search for groundwater based on adequate surface pre-drilling assessment may lead to appreciable ground water yield [5, 32, 37, 38].

Some common surface pre-drilling assessment tools useful in the search for potable groundwater in both sedimentary and basement complex environments are geographic information system (GIS)-based remote sensing

[50, 56] and surface geophysical methods such as electrical resistivity (ER) methods [24, 27]. While GIS-based remote sensing (RS) provides regional overview of the characteristics of geological features [8, 15, 44, 55, 60], electrical resistivity (ER) method delineates geoelectric parameters of the subsurface layers [1, 7, 19, 38, 39, 43, 46].

This is a case study that interprets GIS-based remote sensing and electrical resistivity data to map the groundwater potential in the north-eastern part of Osun State. This is with a view to suggesting sustainable groundwater abstraction in the region. The interpretation involves multi-thematic synthesis [4, 16, 23, 48, 51] of structural elements and aquifer parameters based on analytical hierarchy process (AHP) and multi-criteria decision analysis (MCDA) [6, 48, 50, 54]. This study could form part of the effort to providing for sustainable management of

✉ Dele Falebita, delefalebita@gmail.com | ¹Department of Geology, Obafemi Awolowo University, Ile-Ife, Nigeria. ²Department of Geology, University of Ilorin, Ilorin, Nigeria. ³COPINE, Advanced Space Technology Application Laboratory (ASTAL), Obafemi Awolowo University, Ile-Ife, Nigeria.



groundwater in the basement complex of south-western Nigeria.

2 Study area

The study area lies within longitudes $4^{\circ} 32' 33''$ E to $5^{\circ} 03' 28''$ E and latitudes $7^{\circ} 39' 58''$ N to $8^{\circ} 05' 43''$ N. It is located at the southern part of the Nigerian shield (Fig. 1). This shield is within the pre-drift mobile belt east of the West African and Sao Luis cratons which were affected by the 600 Ma Pan-African orogeny [11–13]. The regional geology is that of the south-western Nigeria's Precambrian basement complex rocks. The basement complex accounts for about 80% of south-western Nigeria's total surface area and has been classified into migmatite-gneiss complexes, meta-sedimentary and meta-volcanic rocks (the schist belts), the Pan-African granitoids (the older granites) and undeformed acid and basic dykes [49]. The local geology shows that the lithology is dominated by metamorphic rocks which include banded gneiss, granite gneiss, schist and quartz schist. Igneous rocks like porphyritic granite and pegmatites are also observed to be present (Fig. 1). It covers seven (7) Local Government areas (LGAs), namely Odo-Otin, Boluwaduro, Ila, Ifedayo, Ifelodun, Boripe, and Obokun LGAs. Osun State is surrounded by five states, namely Kwara state to the north; Ekiti state to the north-east, Ondo state to the south-east, Ogun state to the south-west and Oyo state to the north-west (Fig. 1). The total area is about 2700 square kilometres and easily accessible through network of roads and developed footpaths.

The topography ranges from gentle to steep with ground elevation between 310 and 687 m above sea level and characterized by hills and valleys of varying heights. The area falls within the tropical rainforest type characterized by short dry season (November–March) and a long, wet season (April–October) with mean annual rainfall of about 1600 mm. Annual mean temperature is between 18 and 33 °C with relatively high humidity (NIMET [29]). The vegetation is the evergreen thick forest with varieties of hardwood timbers and grasses (NIMET [29]). It is drained by river Osun and its tributaries and the drainage pattern is dendritic.

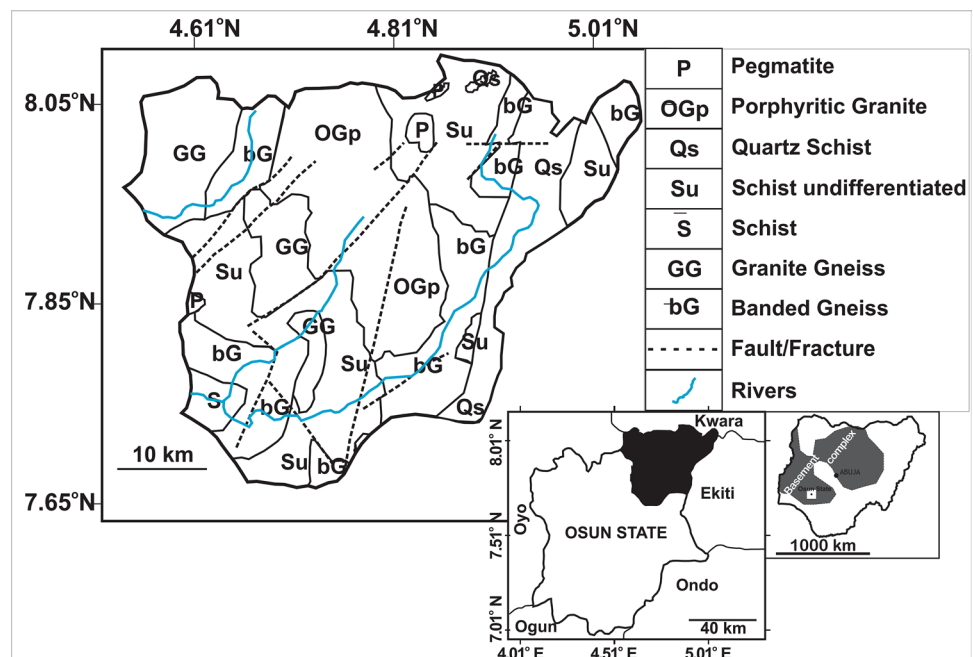
3 Materials and methods

3.1 Materials

The data used in this study are listed below.

1. Administrative map of the study area which showed the Local Government areas (LGAs) of interest were extracted from the Office of the Surveyor General of the Federation (OSGOF) copy of ArcGIS shape file.
2. Geological map of the study area which was acquired from Nigerian Geological Survey Agency (NGSA) [28] and digitized at scale 1:250,000.
3. Landsat 8 operational land imageries (OLI) satellite imagery (Path/row: 190/055), acquired on 05 January 2015, 30 m resolution, which were downloaded

Fig. 1 The study area at the southern part of the Nigerian basement complex showing the distribution of rock units (after [28, 34])



from United States Geological Survey (USGS) website (glovis.usgs.gov) as raw bands 1–8 GeoTIFF files.

4. Subsets of Shuttle Radar Topography Mission (SRTM) imageries (N07_E004, N07_E005, N08_E004, N08_E005), 1 Arc-Second resolution, version 3.2, acquired on 11-FEB-2000 and published on 23-SEP-2014, which were downloaded from: USGS website (glovis.usgs.gov) as GeoTIFF files.
5. One hundred and sixty-four (164) secondary vertical electrical sounding (VES) geophysical data involving the Schlumberger array and a current electrode spacing (AB/2) in the range of 1–150 m were acquired from several sources.

3.2 Extracting lineaments

The ENVI© 5.0, PCI Geomatica©2013 and ArcGIS©10.3 softwares were used to carry out lineament extraction processes. The Band 6 image [21] of the short wave infrared range of the electromagnetic spectrum (SWIR) which is suitable for geological studies was subjected to contrast stretching (histogram equalization), spatial filtering and high pass (edge enhancement) by employing the 3×3 kernel convolution and median filters successively [25, 57]. These were done in order to enhance specific linear trends of higher spatial frequencies and improve visualization for lineament extraction [20, 60]. Moreover, hillshade analysis (spatial analysis) was carried out on the shuttle radar topographic mission (SRTM) image to create an enhanced shaded relief from a surface raster by considering the illumination source angle and shadows at different azimuths [17]. False colour composite (FCC) technique was used to enhance the interpretability of the resulting image because optimal geologic information depiction in FCC imageries relies upon the selection of the three most suitable channels [53]. The extracted lineaments were superimposed on the FCC of bands 6, 4, 2 [21], and those corresponding to unwanted features such as drainage, river

Table 2 Statistics of the depth sounding curves

Curve type	Frequency	%Frequency
A	9	5.488
AKH	6	3.659
H	14	8.537
HA	23	14.024
HAKH	1	0.610
HKH	31	18.902
HKHK	3	1.829
KH	51	31.098
KHA	2	1.220
KHKH	2	1.220
KQH	4	2.439
QH	16	9.756
QHA	2	1.220
Total	164	100

channels, roads, settlements and other man-made features were deleted in order to be left with the hydrogeologically significant lineaments [10]. The extracted Landsat OLI hydrolineaments and SRTM topographic lineaments were merged to produce the remotely sensed lineaments (RSL) map (Fig. 3) [17, 60]. Table 1 shows the statistics of the hydrolineaments. The RSL map (Fig. 3) was then subjected to lineament density (Fig. 4a), intersection density (Fig. 4b) and slope analyses (Fig. 4c). The hydrolineament statistics of orientation, frequency and length is presented in Table 1.

3.3 Extracting geoelectric parameters

Using ArcMap© 10.3, one hundred and sixty-four (164) vertical electrical sounding (VES) stations were georeferenced and interpreted. The VES data were presented as depth sounding curves (Table 2) and interpreted quantitatively using the partial curve matching technique. The

Table 1 Hydrolineament statistics

Lineament orientation	Frequency (F)	Contribution (%)	Minimum length (m)	Maximum length (m)	Mean length	Median length (m)
N–S	24	0.58	129	1249	394.67	298.50
NNE–SSW	888	21.57	90	2490	442.09	381.00
NE–SW	58	1.41	131	1754	312.38	350.50
ENE–WSW	1354	32.90	74	2919	430.54	348.00
NNW–SSE	605	14.70	116	1715	375.06	336.00
NW–SE	28	0.68	140	1448	390.50	340.00
WNW–ESE	1077	26.17	86	2134	346.96	304.00
E–W	82	1.99	103	563	259.16	232.00
Total	4116	100%				

estimated geoelectric parameters of layer resistivities and thicknesses were refined by using them as starting model parameters in a one-dimensional (1D) forward modelling using WinResist© version 1.0 iterative software [58]. The iterated results were used to identify the aquifers (Table 3), evaluate and generate thematic maps of the overburden thicknesses (Fig. 5a), coefficient of anisotropy, λ (Fig. 5b) and the bedrock elevation (Fig. 5c). The processes involved in the derivation of λ for each VES point are shown below:

$$\text{Longitudinal unit conductance (S) in mhos} = \sum_{i=1}^n \frac{h_i}{\rho_i} \quad (1)$$

$$\text{Traverse unit resistance (T) in } \Omega\text{m}^2 = \sum_{i=1}^n h_i \rho_i \quad (2)$$

where h_i and ρ_i are thickness and resistivity, respectively, of the aquiferous layer and $i = 1$ to n represent the 1st to n th layer in which each layer constitutes the aquifer.

$$\text{Electrical coefficient of anisotropy } (\lambda) = \frac{\sqrt{TS}}{H} \quad (3)$$

where $H = h_1 + h_2 + \dots + h_n$ (i.e. the sum of the thicknesses of the layers used to derive S and T). S , T and λ are also known as Dar-Zarrouk parameters. λ is dimensionless, and the value range is ≥ 1 [39].

3.4 Multi-thematic synthesis

Figure 2 describes the synthesis of the groundwater conditioning parameters from remote sensing and electrical resistivity methods to generate the groundwater potential index map of the study area. The parameters are lineament density, lineament intersection density, slope, lithology, electrical coefficient of anisotropy and bedrock elevation thematic maps. These thematic maps were imported into ArcMap© 10.3 model builder engine where the reclassification and weighted-overlay processes were carried out. The weighted-overlay process (synthesis) was then used to combine all the reclassified thematic maps (Figs. 4, 5) into

Table 3 Aquifer type, resistivity and thickness

S. no.	Aquifer type	Resistivity (Ωm)			Thickness (m)		
		Minimum	Maximum	Mean	Minimum	Maximum	Mean
1.	Weathered basement (WB)	4	1108	141.9	0.1	121.9	12.8
2.	Partly weathered/fractured basement (PWFB)	25	2575	309	1.8	120.0	17.3

Fig. 2 Workflow of the multi-variate integration of thematic maps

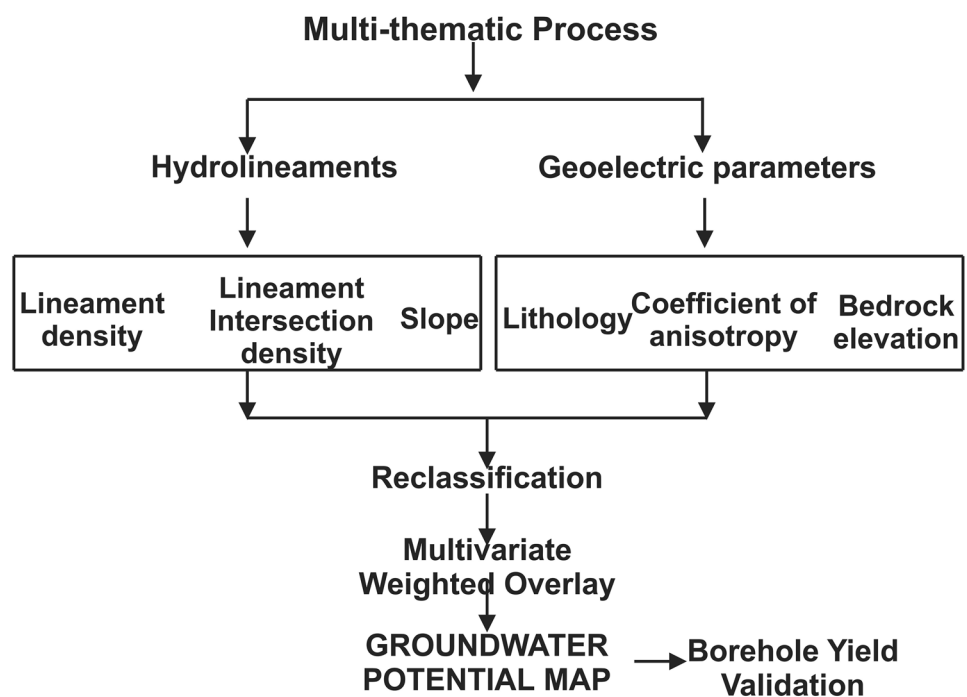


Fig. 3 Hydrolineament map with superposed geology as described in Fig. 1

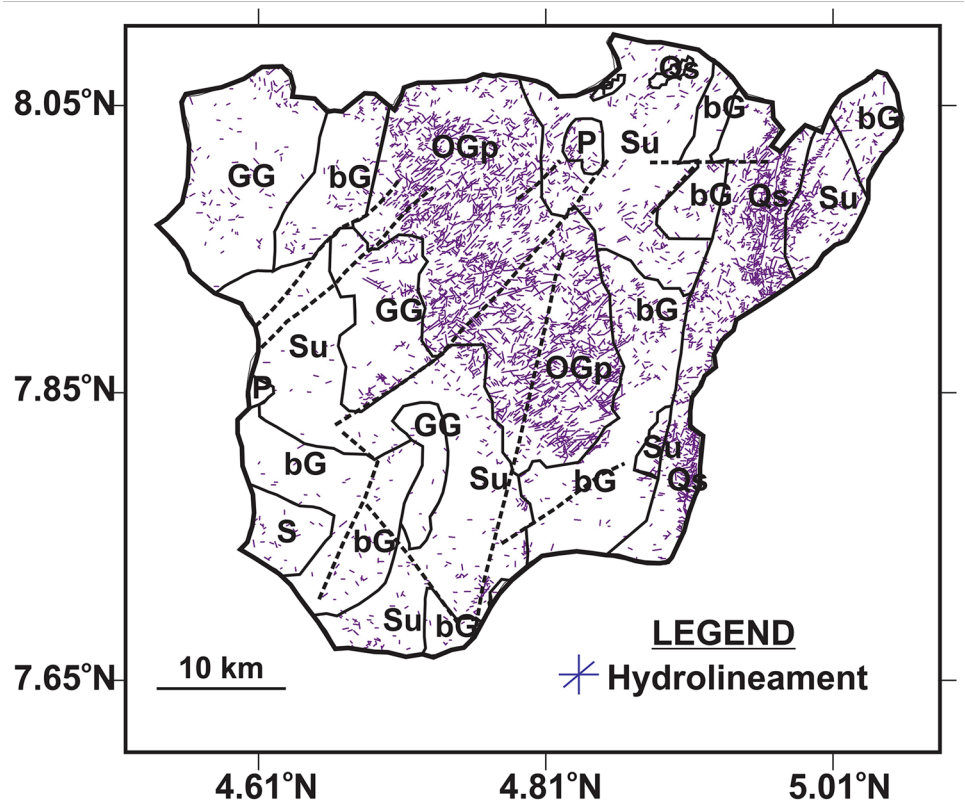
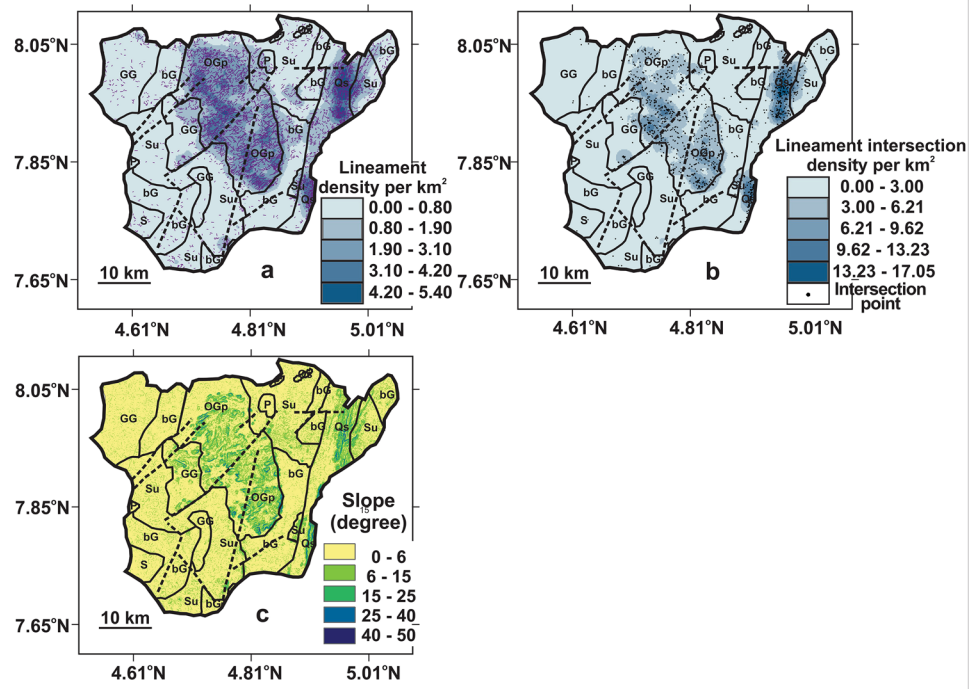


Fig. 4 Lineament distribution **a** lineament density per square kilometre, **b** lineament intersection density per square kilometre and **c** slope



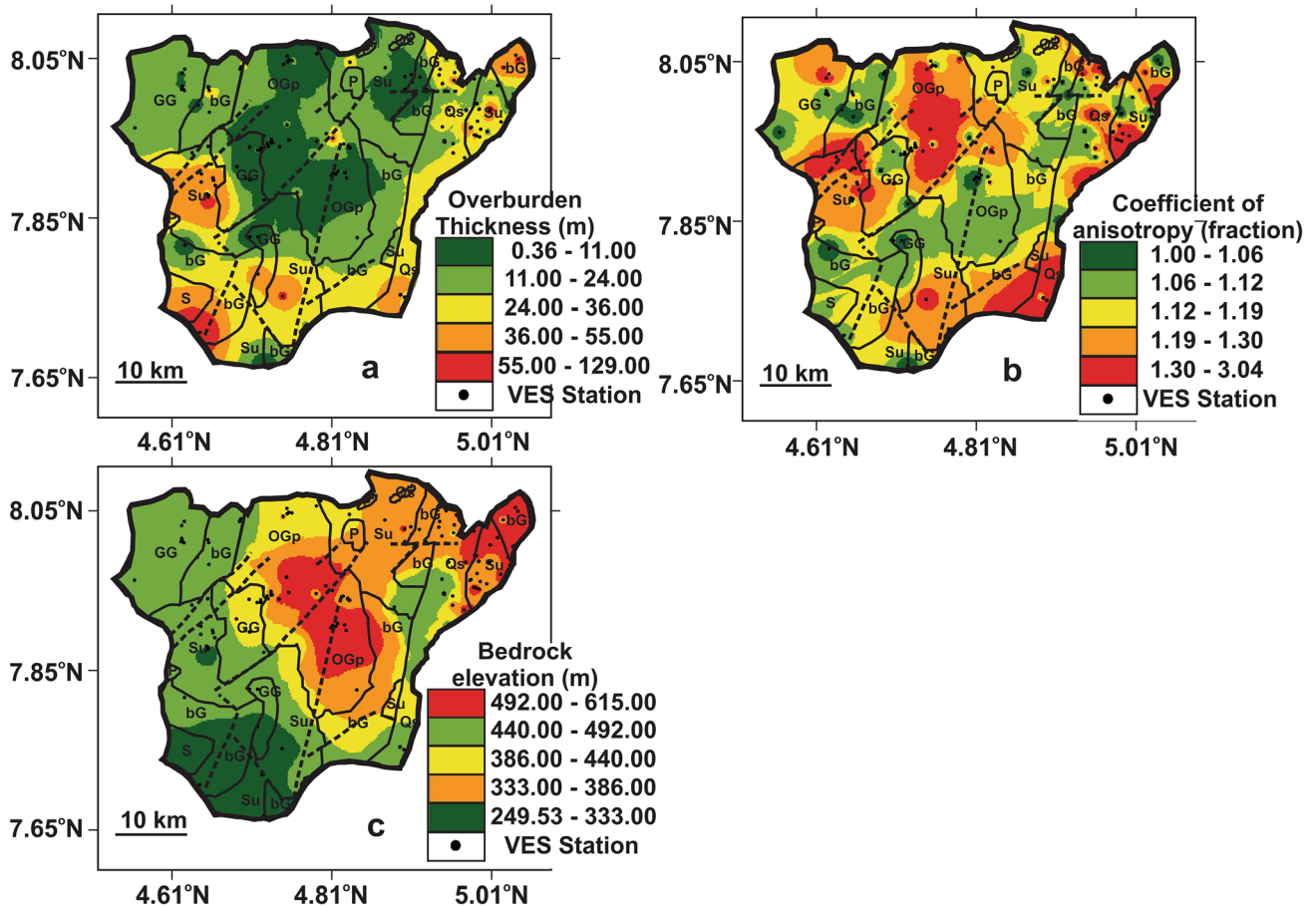


Fig. 5 Geoelectric characteristics **a** overburden thickness, **b** coefficient of anisotropy and **c** bedrock elevation

a final groundwater potential map (Fig. 6) in accordance with the multi-variate equation below:

$$\sum_{i=1}^6 M_i = w_1X_1 + w_2X_2 + w_3X_3 + w_4X_4 + w_5X_5 + w_6X_6 \quad (4)$$

where M is the value for each pixel of the final groundwater potential map of the study area. Variables w_1, w_2, w_3, w_4, w_5 and w_6 are the weight values for each thematic factor and variables X_1, X_2, X_3, X_4, X_5 and X_6 are the ratings (Domakinis et al. 2008). The weights were assigned based on analytical hierarchy process (AHP) and multi-criteria decision analysis (MCDA) [6, 54].

4 Discussion of results

4.1 Hydrolineament and slope characteristics

4.1.1 Lineament length and orientation

There are about 4116 hydrolineaments in the remotely sensed lineament map (Fig. 3) distributed across the rock units (Table 1). Visual inspection indicates that the lineament distribution is concentrated on the porphyritic granite and quartz schist. The lineament lengths vary from less than 100 m to more than 2900 m with mean length ranging from 259 to 442 m depending on azimuth (Table 1). The lineaments oriented in the ENE–WSW direction dominate the area with frequency of 1354 and contribute 32.90% to the total lineament distribution. This is closely followed by WNW–ESE (26.17%); NNE–SSW (21.57%); and NNW–SSE (14.70%). The minor orientations in combination contribute < 5% to the total lineament distribution. They are the E–W (1.99%), NE–SW (1.41%), NW–SE (0.68%) and N–S (0.56%). These major and minor orientations agree

with the result of [9] and are typical of the basement complex region of Nigeria [30, 45, 47].

4.1.2 Lineament density and intersection density

Figure 4a shows the lineament density per square kilometre map of the study area. It reveals a relatively lower lineament density of 0.00–1.90 per km² in the western, southern and part of the north-eastern zones, while relatively higher lineament density of 1.90–5.40 per km² is observed at the central, eastern, south-eastern and part of north-eastern zones. The highest density values are concentrated in the porphyritic granite and quartz schist. The linear intersection density map (Fig. 4b) shows that relatively higher lineament intersection density of 6.21–17.05 per km² is common in the central, north-eastern and south-eastern parts, while relatively lower intersection density (< 6.21) per km² is observed at the remaining parts. There is a good degree of correlation between the lineament density and lineament intersection density maps in that lineaments are more likely to intersect at regions where there are high lineament densities compared to other parts.

4.1.3 The slope of the study area

The slope of the study area varies from 0° to about 60° (Figure 4c). It is essentially dominated by slope values between 0° and 25°. There are only few slope values higher than the 25°. Relatively higher slope values between 15° and 25° are observed at the central and eastern parts which coincide with areas of increased elevation that are underlain by porphyritic granite, granite gneiss and quartz schist. The other parts have slope less than 15°.

4.2 Geoelectric characteristics

4.2.1 VES curve type, aquifer type, resistivity and thickness

Thirteen VES curve types are present in the study area, namely A, AKH, H, HA, HAKH, HKH, HKHK, KH, KHA, KHKH, KQH, QH and QHA (Table 2). The KH (31%), HKH (19%) and HA (14%) curves are predominant as they account for a total of 64% altogether. The other curve types make up the remaining 36%. The high degree of variation in curve types can be related to the heterogeneity of the geology typical of a basement complex region [6].

Table 3 summarizes the aquifer type, resistivity and thickness ranges in the study area. Two major aquifer units, namely weathered basement (WB) and the partly weathered/fractured basement (PWFB), are identified which are highly significant in terms of groundwater storage in the basement complex [40]. The resistivity of the WB varies between 4 and 1108 Ωm with a mean of 141.9 Ωm, while

that of the PWFB varies between 25 and 2575 Ωm with a mean of 309 Ωm. Similarly, the thickness of the WB varies between 0.1 and 121.9 m with a mean thickness of 12.8 m, while that of the PWFB varies between 1.8 and 120.0 m with a mean of 17.3 m. The frequency of occurrence of the WB is higher than that of the PWFB, meaning that the weathered basement is the main aquifer unit. The resistivity values (< 150 Ωm) of the PWFB are diagnostic of zones with high degree of water saturation and significant thickness [2].

4.2.2 Overburden thickness

The overburden thickness varies from as small as 0.36 m to as high as 129 m (Fig. 5a). Thickness range of 0.4–24 m is observed at the central, northern and north-western parts, underlain mostly by porphyritic granite, granite gneiss, banded gneiss and pegmatite rocks. Overburden thickness of 24 m and above is observed at the north-eastern, southern and western parts of the study area, underlain mostly by schist undifferentiated and quartz schist. Schist is known to be characterized by relatively high degree of weathering and may have a strong influence on the observed overburden thickness. In general, thick overburden with little or no clay contents usually favours higher groundwater occurrence [36].

4.2.3 Coefficient of anisotropy

The coefficient of anisotropy (λ) varies between 1.00 and 3.04 (Fig. 5b). The distribution is a reflection of the degree of fracturing and or inhomogeneity in the subsurface and has been found to be related to groundwater yield [3, 39]. In a typical basement terrain, this electrical effect is due to near surface features such as variable degree of weathering and structural features like faults, fractures, joints, foliations and beddings which are in turn responsible for creating secondary porosity that enhances groundwater yield [33]. The anisotropy values (1.19–3.04) observed at the northern, north-eastern, eastern and south-eastern parts correlate well with the remotely sensed lineaments density/intersection locations (Fig. 4a, b). These results agree with the values obtained for areas underlain by metamorphic rocks in the south-western part of Nigeria [39].

4.2.4 Bedrock elevation

Figure 5c shows the bedrock elevation. It is the difference between the overburden thickness and the surface topography. It varies from about 249 m at the southern part to about 615 m at the central to north-eastern parts across rock boundaries. The maximum difference in elevation is about 366 m. The highest (ridge) elevation ranges

between 492 and 615 m and occurs in the porphyritic granite at the central part, while the lowest (depression) elevation ranges between 249 and 333 m and occurs in the schist, banded gneiss and undifferentiated schist at southern part. It is expected that the depressions should favour accumulation of groundwater except the effects of other factors (e.g. fractures) are significant [3].

4.3 Multi-thematic ground water potential

4.3.1 Weight and rating of factors

The reciprocal matrix of pairwise comparison between variables based on AHP [6, 54] is presented in Table 4. It considers the relative contribution of two factors per time. It is a precursor to the relative weight determination between variables (Table 5) where the weights per column sum to 1. The eigenvector is the average weight of the contributing variables per row (Table 5). The consistency ratio (CR) is 0.02 (2%) which is far less than the required 10% threshold which makes it acceptable [22, 54]. Consistency ratio (CR) is the ratio of consistency index (CI) to random index (RI) for the same order matrices [22].

The attribute ratings and factor weighting [10, 35, 44] are presented for in Table 6 for each of the six (6) groundwater potential contributing factors, namely (1) lineament density, (2) lithology, (3) lineament intersection density (4)

electrical coefficient of anisotropy, (5) slope and (6) bedrock elevation. Lineament density is a measure of quantitative frequency of linear feature per unit area which can indirectly reveal the groundwater potential [44, 52]. The high density of lineaments and intersection points allow for connected fractures that are favourable for the accumulation and ease of movement of groundwater [17, 31]. So, areas with higher lineament density and higher lineament intersection density have higher groundwater potential ratings (Table 6). The effective porosity of the two aquifers identified in this study, namely weathered and partly weathered/fractured basement [40, 43] determines the storage capacity, whereas their permeability, determines the groundwater yield [35, 41, 42]. On these bases, areas with lithologies having higher tendencies for degree of fracturing are assigned higher groundwater potential ratings (Table 6). The degree of fracturing or inhomogeneity can also be established through the determination of electrical coefficient of anisotropy (λ) which has been found to be related to groundwater yield [39]. So, areas with higher λ are assigned higher groundwater potential rating. Furthermore, areas with less slope are assigned higher groundwater rating than areas with high slope because the low-slope area limits surface runoff and allows more time for infiltration of rainwater, while high-slope area enhances high runoff with short residence time for infiltration and recharge [44]. Finally, areas where

Table 4 Pairwise comparison matrix table for the thematic indices

	Lineament Density	Lithology	Lineament Intersection	Anisotropy	Slope	Bedrock elevation
Lineament Density	1.00	2.00	3.00	4.00	5.00	6.00
Lithology	0.50	1.00	2.00	3.00	4.00	5.00
Lineament Intersection	0.33	0.50	1.00	2.00	3.00	4.00
Anisotropy	0.25	0.33	0.50	1.00	2.00	3.00
Slope	0.20	0.25	0.33	0.50	1.00	2.00
Bedrock elevation	0.17	0.20	0.25	0.33	0.50	1.00
Sum	2.45	4.28	7.08	10.83	15.50	21.00

Table 5 Determination of relative weights (eigenvectors) for the thematic indices

	Lineament density	Lithology	Lineament intersection	Anisotropy	Slope	Bedrock elevation	Eigenvector
Lineament Density	0.4082	0.4669	0.4235	0.3692	0.3226	0.2857	0.3794
Lithology	0.2041	0.2335	0.2824	0.2769	0.2581	0.2381	0.2488
Lineament Intersection	0.1361	0.1167	0.1412	0.1846	0.1935	0.1905	0.1604
Anisotropy	0.1020	0.0778	0.0706	0.0923	0.1290	0.1429	0.1024
Slope	0.0816	0.0584	0.0471	0.0462	0.0645	0.0952	0.0655
Bedrock elevation	0.0680	0.0467	0.0353	0.0308	0.0323	0.0476	0.0434
Sum	1.0000	1.0000	1.0000	1.0000	1.0000	1.0000	1.0000

Consistency ratio = 0.02 (acceptable)

Table 6 Multi-thematic parameters for the generation of groundwater potential index map

S. no.	Thematic indices	Attribute	Rating	Potential	Normalized weight (w)
1	Lineament density	0.00–0.80	1	Very low	0.3794
		0.80–1.90	2	Low	
		1.90–3.10	3	Moderate	
		3.10–4.20	4	High	
		4.20–5.40	5	Very high	
2	Lithology	Banded gneiss	2	Low	0.2488
		Granite gneiss	2	Low	
		Schist	3	Moderate	
		Porphyritic Granite	3	Moderate	
		Quartz schist	4	High	
3	Lineament intersection density	0.00–3.00	1	Very low	0.1604
		3.00–6.21	2	Low	
		6.21–9.62	3	Moderate	
		9.62–13.23	4	High	
		13.23–17.05	5	Very high	
4	Coefficient of anisotropy	1.00–1.06	1	Very low	0.1024
		1.06–1.12	2	Low	
		1.12–1.19	3	Moderate	
		1.19–1.30	4	High	
		1.30–3.04	5	Very high	
5	Slope	40–60	1	Very low	0.0655
		25–40	2	Low	
		15–25	3	Moderate	
		6–15	4	High	
		0–6	5	Very high	
6	Bedrock elevation	Ridges	1	Very low	0.0434
		Flat	3	Moderate	
		Depressions	5	High	

depressions are observed are assigned higher groundwater potential ratings as they tend to favour the accumulation of groundwater, while areas characterized by ridges are assigned lower ratings (Table 6).

4.3.2 Groundwater potential (*M*) index map

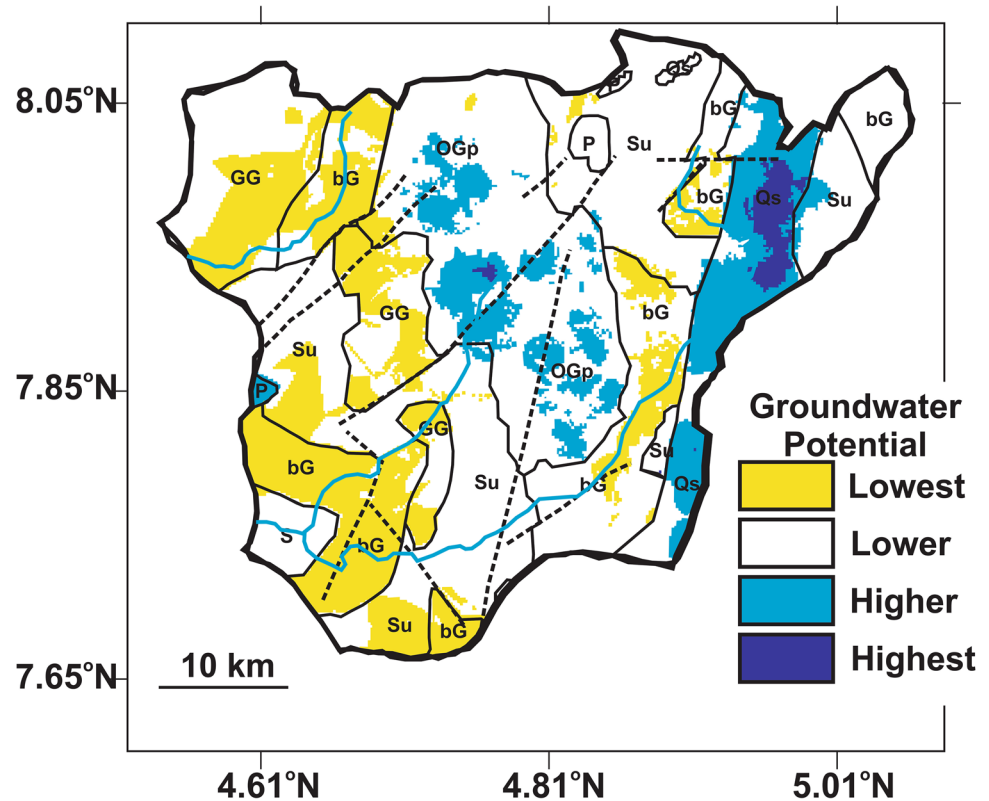
The groundwater potential index map based on Eq. 4 discussed in Sect. 3.4 is presented in Fig. 6, where *w* is the weight and *X* is the rating of the six contributing factors—lineament density, lithology, lineament intersection density, electrical coefficient of anisotropy, slope and bedrock elevation indexed from 1 to 6, respectively. It is calibrated in a relative term for the study area into the highest, higher, lower and lowest groundwater potential distribution across the rock units. Lowest to lower potential covers more areas that are principally associated with undifferentiated schist, granite gneiss and banded gneiss, while higher to highest potential covers less areas associated with porphyritic granite and quartz schist (Fig. 6).

This distribution is greatly influenced by the lineament density and intersection density (Fig. 4a, b), and it is probably related to the fact that pegmatitic and quartzitic rocks have the tendency for higher degree of accumulation and movement of groundwater due to fracturing than meta-sediments (schist) and charnockitic rocks [40, 43].

4.3.3 Validation with borehole yields

Yield can be regarded as borehole information which is a reflection of the different but integrated groundwater controlling factors in a particular place. It is the ultimate interest in any groundwater study. Figure 7a shows the distribution of the borehole yields in litres per second (l/s) obtained through pumping test of 48 available boreholes in the study area. It is roughly classified into four categories as the groundwater potential index map for comparison (Fig. 7b). It can be observed that the groundwater yield varies between 1.03 and 1.60 l/s and is distributed randomly across the study area. This distribution

Fig. 6 Multi-thematic ground-water potential index map



offers some gross classification of the potential map constrained by the yields (Fig. 7b). For example, the yield values between 1.03 and 1.22 l/s are associated with lowest potential, while 1.35 and 1.60 l/s are associated with the highest potential. The lower potential is associated with yield values between 1.22 and 1.29 l/s, while the higher potential is associated with the yields between 1.29 and 1.35 l/s. The yields between 1.29 and 1.60 l/s occupy less areas and are concentrated at the central to the eastern parts, while yields between 1.03 and 1.29 l/s occupy more areas and distributed everywhere else. So, we posit that the expected yield is grossly between 1.03 and 1.60 l/s and that the groundwater potential index map is a reflection of the groundwater distribution in the region until more data become available.

4.4 Sustainable management of groundwater

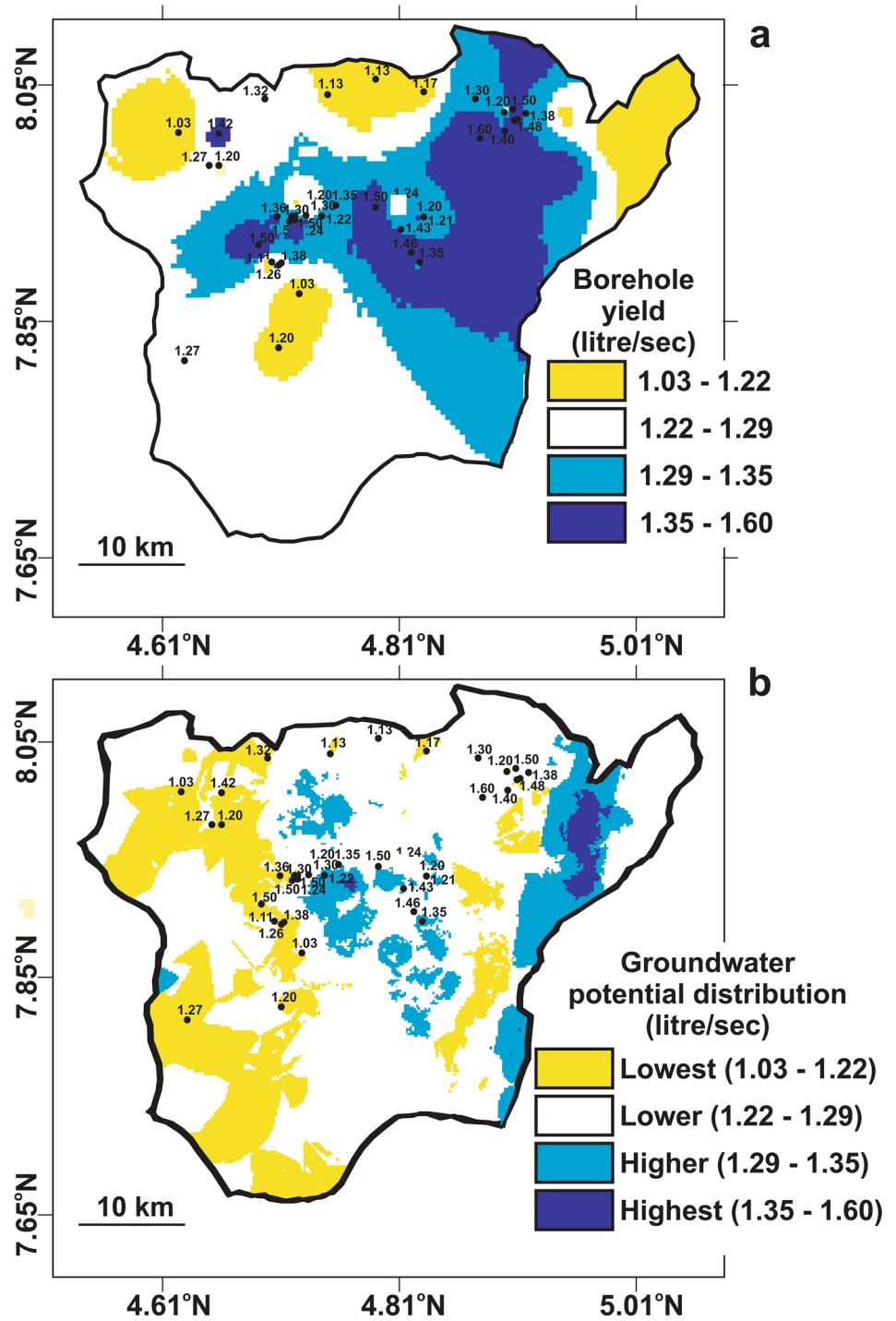
This study attempts to go beyond high and low potential classification because we know that variations in borehole yields may affect the purpose of abstraction of water. This was achieved by analysing the groundwater yields in term of quantity of water that can be abstracted within a particular time-frame. For example, all things being equal as in Fig. 7, the lowest yield rate of 1.03 l/s in the study area is equivalent to 3708 l/h. This is a little above three-and-half 1000 l tanks in 1 h, which may be enough for domestic

uses in a single location for 1 day. Similarly, the highest yield of 1.60 l/s is equivalent to 5760 l/h which is just about two 1000 l tanks above the lowest yield. So, for sustainable management, the groundwater resource in the region may only be suitable and enough for domestic uses and probably small-to-medium-scale agriculture and industries whose needs for potable water are relatively limited.

5 Conclusion

This study describes the application of GIS-based remote sensing and electrical resistivity geophysical methods using a multi-thematic synthesis of structural and aquifer parameters in a basement complex area where there is a high demand for groundwater for domestic, industrial and intensive agriculture uses. Six important groundwater conditioning factors, namely lineament density, lineament intersection density, slope, lithology, electrical coefficient of anisotropy and bedrock elevation, were synthesized. The synthesis was based on the analytical hierarchy process (AHP) and multi-criteria decision analysis (MCDA) to produce groundwater potential index which was validated by existing borehole yields. The results indicate some gross degree of agreement between the distribution of the borehole yields and the groundwater potential index map and can serve as a rough predictor of the groundwater

Fig. 7 **a** Distribution of borehole yields and **b** ground-water distribution potential constrained by yields



distribution in region. In addition, the distribution of the borehole yields suggests that the groundwater in the region may only be suitable for domestic uses as well as the use of small-to-medium-scale agriculture and industries. The suggestions from this study could guide further town planning and land use decisions for sustainable management of groundwater abstraction in the study area.

Acknowledgements The authors thank the Federal Survey of Nigeria, Nigerian Geological Survey Agency and Advanced Space Technology Application Laboratory (ASTAL), Obafemi Awolowo University, Ile-Ife, Nigeria, for providing the administrative map, geological map and GIS data, respectively, and also the United States Geological Survey for the use of the Landsat 8 operational land imageries (OLI) satellite imagery data. We acknowledge the numerous private and

public sources of the VES geophysical data as well as the anonymous reviewers.

Compliance with ethical standards

Conflict of interest On behalf of all authors, the corresponding author states that there is no conflict of interest.

References

- Abiola O, Enikanselu PA, Oladapo MI (2009) Groundwater potential and aquifer protective capacity of overburden units in Ado-Ekiti, Southwestern Nigeria. *Int J Phys Sci* 4(3):120–132
- Ademilua OL (1997) A geoelectric and geologic evaluation of groundwater potential of Ekiti and Ondo States, Southwestern, Nigeria. Unpublished M.Sc. thesis, Department of Geology, Obafemi Awolowo University, Ile-Ife, Nigeria, pp 1–67
- Adepelumi AA, Akinmade OB, Fayemi O (2013) Evaluation of groundwater potential of Baikin Ondo State Nigeria using resistivity and magnetic techniques: a case study. *Univ J Geosci* 1(2):37–45
- Adiat K, Nawawi M, Abdullah K (2012) Assessing the accuracy of GIS-based elementary multi criteria decision analysis as a spatial prediction tool: a case of predicting potential zones of suitable ground water resources. *J Hydrol* 440–441:75–89
- Ajayi O, Abegunrin OO (1994) Borehole failures in crystalline rocks of South-Western Nigeria. *Geojournal* 34(4):397–405. <https://doi.org/10.1007/BF00813135>
- Akinlalu AA, Adegbuyiro A, Adiat KAN, Akeredolu BE, Lateef WY (2017) Application of multi-criteria decision analysis in prediction of groundwater resources potential: a case of Oke-Ana, Ilesa Area Southwestern, Nigeria. *NRIAG J Astron Geophys* 6:184–200
- Ako BD, Osondu VC (1986) Electrical resistivity survey of the Kerri-Kerri Formation, Darazo, Nigeria. *J Afr Earth Sci* 5(5):527–534
- Amadi AN, Olasehinde PI (2010) Application of remote sensing techniques in hydrogeological mapping of parts of Bosso Area, Minna, North-Central Nigeria. *Int J Phys Sci* 5:1465–1474
- Ayodele OS, Odeyemi IB (2010) Analysis of the lineaments extracted from LANDSATMM image of the area around Okemesi, South-Western Nigeria. *Indian J Sci Technol* 3:31–36
- Bayowa OG, Olorunfemi MO, Akinluyi OF, Ademilua OL (2014) A preliminary approach to the groundwater potential appraisal of Ekiti State, Southwestern Nigeria. *Int J Sci Technol* 4(3):301–308
- Black R, Liegeois JP (1993) Cratons, mobile belts, alkaline rocks and continental lithospheric mantle—the Pan-African testimony. *J Geol Soc Lond* 150:89–98
- Burke KC, Dewey JF (1972) Orogeny in Africa. In: Dessauvage TFJ, Whiteman AJ (eds) *African geology*. University of Ibadan, Ibadan, pp 583–608
- Caby R, Bertrand JM, Black R (1981) Pan-African closure and continental collision in the Hoggar-Iforas segment central Sahara. In: Kroner A (ed) *Precambrian plate tectonics*. Elsevier, Amsterdam, pp 407–434
- Carla AC, Miriam RS, John SG (2010) Lineament mapping for groundwater exploration using remotely sensed imagery in Karst Terrains. Michigan Technological University, 1400 Townsend Drive, Houghton, MI 49931. GSA annual meeting, Poster # 146
- Chowdhury A (2006) Evaluation of groundwater potential in West Medinipur district using remote sensing and GIS. Unpublished Ph.D. thesis, IIT Kharagpur, p 188
- Chowdhury A, Jha MK, Chowdary VM, Mal BC (2009) Integrated remote sensing and GIS-based approach for assessing groundwater potential in West Medinipur district, West Bengal India. *Int J Remote Sens* 30(1):231–250
- Constant C, Orimoogunje OOI, Hlatywayo DJ, Akinyede JO (2013) Application of remote sensing and geographical information systems in determining the groundwater potential in the crystalline basement of Bulawayo Metropolitan Area, Zimbabwe. *Adv Remote Sens* 2:149–161
- Chen X (1992) Application of remote sensing and GIS techniques for environmental geologic investigation, Northeast Iowa. Ph.D. thesis, University of Iowa, Iowa, Iowa, USA
- Emenike EA (2000) Geophysical exploration for groundwater in a sedimentary environment: a case study from Nanka over Nanka Formation in Anambra Basin, Southeastern Nigeria. *Glob J Pure Appl Sci* 7(1):97–110
- GeoInfo (2016) <http://geoinfo.amu.edu>. Accessed 10 Aug 2016
- GeoSpatial (2015) <http://www.info-geospasial.com/2015/07/kombinasi-band-citra-landsat-8.html>. Accessed 17 Aug 2016
- Ho W (2008) Integrated analytic hierarchy process and its applications—a literature review. *Eur J Oper Res* 186(1):211–228
- Jha MK, Chowdary VM, Chowdhury A (2010) Groundwater assessment in Salboni Block, West Bengal (India) using remote sensing, geographical information system and multi-criteria decision analysis techniques. *Hydrogeol J* 18:1713–1728
- Mansour AAG (2009) Geophysical investigations for groundwater in a complex subsurface terrain, Wadi Fatima, KSA: a case history. *Jordan J Civ Eng* 3(2):91–100
- Matt D, Lewis P (2006) Online course module on spatial filtering using ENVI. <http://www2.geog.ucl.ac.uk/~mdisney/teaching/2021/practical>
- Meijerink AMJ (2007) Remote sensing applications to groundwater. IHP-VI series on groundwater, Paris, UNESCO, 16
- Mohamaden MII, Hamouda AZ, Mansour S (2016) Application of electrical resistivity method for groundwater exploration at the Moghra area, Western Desert, Egypt
- Nigeria Geological Survey Agency (2006) Geological Map of Osun State, Nigeria. NGSA, Abuja
- Nigeria Meteorological Agency (NIMET) (2007) Daily weather forecast on the Nigerian television authority. Nigerian Meteorological Agency, Oshodi, Lagos
- Odeyemi IB, Asiwaju-Bello YA, Anifowose AYB (1999) Remote sensing fracture characteristics of the Pan African granite batholiths in the basement complex of parts of Southwestern Nigeria. *J Techno-Sci* 3:56–60
- Odeyemi IB, Malomo S, Okufarasin YA (1985) Remote sensing of rock fractures and groundwater development success forum, United Nations, New York. *J Am Earth Sci* 9(4):311–315
- Offodile ME (1983) The occurrence and exploitation of groundwater in Nigerian Basement Rocks. *Niger J Min Geol* 20(1&2):131–146
- Ogungbemi OS, Badmus GO, Ayeni OG, Ologe O (2013) Geoelectric investigation of aquifer vulnerability within Afe Babalola University, Ado-Ekiti, Southwestern Nigeria. *IOSR J Appl Geol Geophys IOSR-JAGG* 1(5):78–89
- Ojo JS, Olorunfemi MO, Falebita DE (2011) An appraisal of the geologic structure beneath the Ikogosi warm spring in south-western Nigeria using integrated surface geophysical methods. *Earth Sci Res J* 15(1):27–34
- Ojo JS, Olorunfemi MO, Akintorinwa OJ, Bayode S, Omosuyi GO, Akinluyi FO (2015) GIS integrated geomorphological, geological and geoelectrical assessment of the groundwater potential of Akure Metropolis, Southwest Nigeria. *J Earth Sci Geotech Eng* 5(14):85–101

36. Okhue ET, Olorunfemi MO (1991) Electrical resistivity investigation of a typical basement complex area—the Obafemi Awolowo University Campus Case Study. *J Min Geol* 27(2):63–69
37. Olayinka AI, Mbachi CNC (1992) A technique for the interpretation of electrical sounding from crystalline basement areas of Nigeria. *J Min Geol* 27:63–69
38. Olayinka AI, Olorunfemi MO (1992) Determination of geoelectrical characteristics in Okene area and implication for borehole siting. *J Min Geol* 28:403–412
39. Olorunfemi MO, Olarewaju VO, Alade O (1991) On the electrical anisotropy and groundwater yield in a basement complex area of Southwestern Nigeria. *J Afr Earth Sci* 12(3):467–472
40. Olorunfemi MO, Fasuyi SA (1993) Aquifer types and the geoelectric/hydrogeologic characteristics of part of the central basement terrain of Nigeria (Niger State). *J Afr Earth Sci* 16(3):309–317
41. Olorunfemi MO (2008) Voyage on the skin of the earth: a geophysical experience. An inaugural lecture delivered at the Obafemi Awolowo University, Ile-Ife, Nigeria, Tuesday, 11 March, 2008, inaugural lecture series 211, Obafemi Awolowo University Press Ltd, Ile-Ife, Nigeria, pp 1–2
42. Olorunfemi MO, Ojo JS, Akintunde MO (1999) Hydro-geophysical evaluation of the groundwater potential of the Akure Metropolis, Southwestern Nigeria. *J Min Geol* 35(2):207–229
43. Olorunfemi MO, Olorunniwo MA (1985) Geoelectric parameters and aquifer characteristics of some parts of Southwestern Nigeria. *Geol Appl Idrogeol* 10:99–109
44. Olutoyin AF, Moshood NT, Abel OT, Oluwatola IA (2014) Delineation of groundwater potential zones in the crystalline basement terrain of SW-Nigeria: an integrated GIS and remote sensing approach. *Appl Water Sci* 4:19–38
45. Oluyide PO (1988) Structural trends in Nigeria Basement Complex. In: Precambrian geology of Nigeria. Geological Survey of Nigeria Publication, pp 93–98
46. Oseji JO, Ujuanbi O (2009) Hydrogeophysical investigation of groundwater potential in Emu Kingdom, Ndokwa land of Delta State, Nigeria. *Int J Phys Sci* 4(5):275–284
47. Owoyemi FB (1996) A geologic-geophysical investigation of rain-induced erosional features in Akure Metropolis. Unpublished M.Sc. thesis, Federal University of Technology, Akure, pp 11–18
48. Popoola K, Talabi AO, Afolagboye LO, Oyedele AA, Ojo AA (2020) Groundwater potential evaluation in the basement complex terrain of Ekiti East local Government Area, Southwestern Nigeria. *Int J Energy Water Resour* 4:81–90
49. Rahaman MA (2006) Nigeria's solid minerals Endowment and sustainable development in the basement complex of Nigeria and its mineral resources. In: Oshin AK (ed) Jinad & Co., Ibadan, Nig., pp 139–168
50. Rajaveni SP, Brindha K, Elango I (2017) Geological and geomorphological controls on groundwater occurrence in a hard rock region. *Appl Water Sci* 7:1377–1389. <https://doi.org/10.1007/s13201-015-0327-6>
51. Rao YS, Jugran DK (2003) Delineation of groundwater potential zones and zones of groundwater quality suitable for domestic purposes using remote sensing and GIS. *Hydrol Sci J* 48(5):821–833
52. Rao NS, Chakradhar GKJ, Srinivas V (2001) Identification of groundwater potential zones using remote sensing techniques in and around Gunur Town, Andhra Pradesh, India. *J Indian Soc Remote Sens* 29(1–2):69–78
53. Sarp G (2005) Lineament analysis from satellite images, North-West of Ankara. Unpublished M.Sc. thesis, the Graduate School of Natural and Applied Sciences, Middle East
54. Saaty TL (1980) The analytic hierarchy process; planning, priority setting, resource allocation. McGraw-Hill, New York
55. Singhroy VH, Lowman P (2014) Remote sensing and geologic structure. In: Njoku EG (ed) Encyclopedia of remote sensing: encyclopedia of earth sciences series. Springer, New York. <https://doi.org/10.1007/978-0-387-36699-9>
56. Sultan ASA, Josef P (2014) Delineating groundwater aquifer and subsurface structures using integrated geophysical interpretation at the western part of Gulf of Aqaba, Sinai, Egypt. *Int J Water Resour Arid Environ* 3(1):51–62
57. Utsa (2016) <http://www.utsa.edu>. Accessed 20 Sept 2016
58. Vander VBPA (1988) Winresist version 1.0
59. Verma RK, Rao MK, Rao CV (1980) Resistivity investigation for groundwater in metamorphic areas near Dhanbad India. *Groundwater* 18(1):46–55
60. Yenne EY, Anifowose AYB, Dibal HU, Nimchak RN (2015) An assessment of the relationship between lineament and groundwater productivity in a part of the Basement Complex, Southwestern Nigeria. *IOSR J Environ Sci Toxicol Food Technol IOSR-JESTFT* 9(6):23–35

Publisher's Note Springer Nature remains neutral with regard to jurisdictional claims in published maps and institutional affiliations.